ORIGINAL RESEARCH ARTICLE

Amyloid Beta Deregulates Astroglial mGluR5-Mediated Calcium Signaling via Calcineurin and NF-kB

Dmitry Lim,[1] Anand Iyer,[2] Virginia Ronco,[1] Ambra A. Grolla,[1] Pier Luigi Canonico,[1] Eleonora Aronica,[2,3,4] and Armando A. Genazzani[1]

The amyloid hypothesis of Alzheimer's disease (AD) suggests that soluble amyloid β (Aβ) is an initiator of a cascade of events eventually leading to neurodegeneration. Recently, we reported that Aβ deranged Ca^{2+} homeostasis specifically in hippocampal astrocytes by targeting key elements of Ca^{2+} signaling, such as mGluR5 and IP_3R1. In the present study, we dissect a cascade of signaling events by which Aβ deregulates glial Ca^{2+}: (i) 100 nM Aβ leads to an increase in cytosolic calcium after 4–6 h of treatment; (ii) mGluR5 is increased after 24 h of treatment; (iii) this increase is blocked by inhibitors of calcineurin (CaN) and NF-kB. Furthermore, we show that Aβ treatment of glial cells leads to de-phosphorylation of Bcl10 and an increased CaN-Bcl10 interaction. Last, mGluR5 staining is augmented in hippocampal astrocytes of AD patients in proximity of Aβ plaques and co-localizes with nuclear accumulation of the p65 NF-kB subunit and increased staining of CaNAα. Taken together our data suggest that nanomolar [Aβ] deregulates Ca^{2+} homeostasis via CaN and its downstream target NF-kB, possibly via the cross-talk of Bcl10 in hippocampal astrocytes.

Key words: Alzheimer disease; astrocytes; receptors; metabotropic glutamate; NF-kappa B p65

GLIA 2013;00:000–000

INTRODUCTION

Extracellular soluble amyloid β (Aβ) oligomers trigger the so called "amyloid cascade" of events in early Alzheimer's disease (AD) pathogenesis that, with disease progression, leads to neuronal death with concomitant cognitive disturbances (Hardy and Selkoe, 2002). Yet, the exact mechanism by which Aβ initiates cellular deregulation is still a question of debate (Hardy and Selkoe, 2002).

Deregulation of cellular Ca^{2+} homeostasis has been proposed to play a role in the initial steps of disease progression (Thibault et al., 2007). According to the "calcium hypothesis" of AD, a long lasting overload of the cytoplasm and of the endoplasmic reticulum (ER) with Ca^{2+} induces activation of mechanisms leading to cell death (Supnet and Bezprozvanny, 2010). The exact mechanism by which this occurs is still a matter of debate (Demuro et al., 2010; Kagan and Thundimadathil, 2010; Kuchibhotla et al., 2008; Tu et al., 2006). A number of effectors downstream of Ca^{2+} in AD have been proposed, among which the calcium/calmodulin-dependent phosphatase calcineurin (CaN) and its direct downstream target nuclear factor of activated T cell (NFAT) (Abdul et al., 2011; Reese and Taglialatela, 2011).

Glia is an established partner of neurons in the execution and regulation of brain functions, including synaptic transmission. Recent evidence indicates that it may be an important player in AD pathogenesis (Parpura et al., 2012). Reactive astrocytes, present also in normal aging, are found in AD postmortem brains, as well as in animal models, around amyloid plaques (DeWitt et al., 1998). Furthermore, Aβ provokes multiple alterations in glial homeostasis, including

View this article online at wileyonlinelibrary.com. DOI: 10.1002/glia.22502

Published online in Wiley Online Library (wileyonlinelibrary.com)

Received Jan 9, 2013, Accepted for publication Mar 5, 2013.

Address correspondence toGenazzani Armando A. Genazzani, Department of Pharmaceutical Sciences, Università degli Studi del Piemonte Orientale "Amedeo Avogadro," Novara 28100, Italy. E-mail: armando.genazzani@pharm.unipmn.it

From the [1]Department of Pharmaceutical Sciences, Università degli Studi del Piemonte Orientale "Amedeo Avogadro," Novara, Italy; [2]Department of (Neuro)Pathology, Academic Medical Center, University of Amsterdam, Amsterdam, The Netherlands; [3]Stichting Epilepsie Instellingen Nederland (SEIN), Heemstede, The Netherlands; [4]Swammerdam Institute for Life Sciences, Center for Neuroscience, University of Amsterdam, Amsterdam, The Netherlands.

Grant sponsor: Fondazione Cariplo; Grant number: 2008- Grant sponsor: EU FP7 project DEVELAGE; Grant number: 278486.

deregulation of Ca^{2+} signaling (Kuchibhotla et al., 2009), transcriptional changes (Peters et al., 2009), and inflammatory responses (Rubio-Perez and Morillas-Ruiz, 2012).

Recently, using an in vitro Tat-Pro-ADAM10 model of AD (Marcello et al., 2007), we have demonstrated that in astrocytes Aβ produces alterations of Ca^{2+} homeostasis by over-expressing mGluR5 and IP_3R1 at the transcriptional level (Grolla et al., 2013). In the present work, we dissect the molecular mechanism by which Aβ_{42} leads to mGluR5 up-regulation in glia and, as a consequence, Ca^{2+}-deregulation. We now propose that Aβ_{42} leads to cytosolic calcium increases, this leads to CaN activation, which in turn (possibly via Bcl10), activates NF-kB-dependent transcription of mGluR5. IP_3R2 appears to be controlled in a similar manner. We also provide evidence that mGluR5 staining is augmented in hippocampal astrocytes of AD patients in proximity of Aβ plaques and is co-localized with nuclear accumulation of the p65 NF-kB subunit and with increased staining of CaNAα.

MATERIALS AND METHODS

Cell Culture

Primary hippocampal astroglial cell cultures were prepared from postnatal days 1–3 (P1–P3) rat hippocampi as described previously (Fresu et al., 1999). Hippocampal glial cells were seeded in Dulbecco's Modified Eagle's Medium, supplemented with 10% fetal bovine serum, 2 mg/mL glutamine, 10 U/mL penicillin, and 100 μg/mL streptomycin (Sigma, Milan, Italy). Cells were grown until confluence (2–4 days) and then were re-plated for the experiments on plates coated with 0.1 mg/mL poly-L-lysine. The purity of cultures was assayed by immunostaining with anti-MAP2 (neuronal marker) and anti-GFAP (glial marker). No neurons were detected in glial primary cultures.

Aβ Preparation

Aβ 1–42 (Aβ_{42}) was purchased either from Bachem (Bubendorf, Switzerland) or from Innovagen (Lund, Sweden). Aβ_{42} oligomers were prepared as described by Giuffrida et al. (2009) with some modifications. Briefly, the peptide was dissolved in 1,1,1,3,3,3-hexafluoro-2-propanol (HFIP), Fluka Cat. 52512 to 1 mg/mL, monomerized by 1 h incubation at 37°C, lyophilized, resuspended in dimethylsulfoxide (DMSO) at 5 mM, diluted in ice-cold minimum essential medium (MEM) to 100 μM and oligomerized for 24 h at 4°C. The peptide was snap frozen and kept at −80°C. Unless otherwise stated, final concentration of Aβ_{42} was 100 nM.

Antibodies and Drug Treatment

Primary antibodies to: mGluR5 (ab53090, for Western Blot (WB) 1:500) was from Abcam (Cambridge, UK). Anti-IP_3R1 (WB 1:500) antibody was a kind gift from Dr. Colin Taylor (University of Cambridge). Antibodies to p65 (sc-372, for immunocytochemistry (ICC) 1:50), CaNAα (sc-6123, WB 1:200), CaNAβ (sc-6124, WB 1:200), Bcl10 (sc-5611, WB 1:500) were from Santa Cruz (Santa Cruz, CA). Anti-phosphoserine (p-Ser, ALX-804-167, WB 1:1,000) was from Alexis (Enzo Life Sciences, Lausen, Switzerland); anti-β-actin (A1978, WB 1:4,000) was from Sigma. AlexaFluor 488 secondary antibodies were from Life Sciences (Milan, Italy), peroxidase-conjugated secondary antibodies from Pierce (Rockford, IL).

In all experiments, FK506, cyclosporine A, caffeic acid phenethyl ester (CAPE) and 4-methyl-N^1-(3-phenylpropyl)benzene-1,2-diamine (JSH-23, JSH) (all from Sigma, Milan, Italy) were used at 100 nM, 1 μM, 40 μM, and 20 μM, respectively, 1 h before treatment with Aβ_{42}. (*S*)-3,5-Dihydroxyphenylglycine (DHPG), 2-aminoethoxydiphenylborane (2-APB), nifedipine, 6,7-dinitroquinoxaline-2,3-dione (DNQX) (all from Tocris, Bristol, UK) were used at 20 μM, 100 μM, 100 nM, and 30 μM, respectively.

NF-kB Luciferase Assay

About 1×10^5 cells/well were plated in 24-well plates and 12–24 h after plating were transfected with an NF-kB-Luc reporter plasmid (Clontech) using Lipofectamine 2000 (Life Technologies, Milan). Twenty-four hours after transfection, cells were treated with inhibitors and with Aβ_{42} for 12–15 h. Luciferase activity was assayed using Bright-Glo Luciferase Assay System (Promega, Milan, Italy) according to the manufacturer's instruction.

Calcium Imaging

Cells were loaded with Fura-2 AM as described by Grolla et al. (2013). After de-esterification (30 min at room temperature (RT)) the coverslip was mounted in an acquisition chamber and placed on the stage of a Leica epifluorescent microscope equipped with a S Fluor ×40/1.3 objective. Cells were excited alternatively with 340/380 nm using a monochromator Polichrome V (Till Photonics, Munich, Germany), and the fluorescence light, filtered through a band-pass 510 nm filter was collected by cooled CCD camera (Hamamatsu, Japan) and acquired by MetaFluor software. To quantify the differences in the peaks of Ca^{2+} transients the ratio values were normalized using the formula $(F_i - F_o)/F_o$ (referred to as normalized Fura-2 ratio, norm. ratio). The cells with norm. ratio above 0.2 were considered as responders. For baseline Ca^{2+} measurements, cells were treated with Aβ_{42} for 3 h, then 2 μM Fura-2 was added for 30 min directly to culture medium and the cells were transferred to room temperature to avoid Fura-2 compartmentalization. At the end of each recording, cells were perfused with a solution containing 10 μM ionomycin with either 10 mM Ca^{2+} or 25 mM EGTA. Concentrations of Ca^{2+} were calculated according to the work by Grynkiewicz et al. (1985). Data were analyzed using GraphPad Prism Software (San Diego, CA).

Real-Time PCR

Total mRNA was extracted from 7.0×10^5 cells using QIAzol Lysis Reagent (Qiagen, Milan, Italy) according to manufacturer's instructions. First strand of cDNA was synthesised from 1 μg of total RNA using ImProm-II RT system (Promega). Real-time PCR was performed using GoTaq qPCR Master Mix (Promega) on an SFX96 Real-Time System (Biorad, Segrate, Italy). S18 ribosomal protein was used to normalize PCR product levels. Following oligonucleotide primers were used (from 5′ to 3′): S18 (NM_213557) forward

(Forw)-TGCGAGTACTCAACACCAACA, reverse (Rev) CTGCTTTCCTCAACACCACA; mGluR5 (NM_017012) Forw GCCATGGTAGACATAGTGAAGAGA, Rev TAAGAGTGGGCGATGCAAAT; IP3R1 (NM_001007235) Forw GGCTACAGAGTGCCTGACCT, Rev CCATTCGTAGATCCCTCTGC; IP3R2 (NM_031046) Forw TCCAAAAGACGTTGGACACA, Rev TTCATCCCCTTCCTCTGGAT.

Immunocytochemistry

Twenty-four hours before treatment, 5×10^4 glial cells were plated onto 13 mm coverslips in 24-well plates. Treated cells were fixed in 4% formaldehyde in PBS for 15 min at RT, permeabilized for 7 min in PBS with 0.1% Triton X-100 and blocked for 30 min in 2% gelatine. Then primary (1 h, 37°C) and secondary (1 h, RT) antibody were applied in PBS with 2% gelatin. After washing (3×5 min), nuclei were stained with 4′,6-diamidino-2-phenylindole dihydrochloride (DAPI) for 15 min at RT. Fluorescence images were acquired using a Leica epifluorescent microscope equipped with S Fluor ×40/1.3 objective using MetaMorph software.

Immunoprecipitation and Western Blot

For immunoprecipitation (IP), $3–5 \times 10^5$ glial cells were plated in 60-mm Petri dishes. On the day of experiment, cells were pretreated with inhibitors and then treated with $A\beta_{42}$ for 6 h. Cells were then scraped on ice in 300 μl IP buffer (50 mM Tris-HCl, pH = 7.4, 150 nM NaCl, 1% NP-40) supplemented with protein inhibitors cocktail (PIC), 0.1 mM phenylmethanesulfonylfluoride (PMSF), and phosphatase inhibitors cocktail (all from Sigma), quantified with Micro BCA Protein Assay Kit (Pierce, Rockford, IL). About 500 μg of total proteins were immunoprecipitated using A/G agarose beads (Santa Cruz Biotechnology, Santa Cruz, CA) according to manufacturer's instructions with 2 μg primary anti-Bcl10, anti-CnAα, or anti-CnAβ antibodies in 0.5 mL at 4°C O/N on a rotator shaker. After intensive washing, precipitates were dissolved in 100 μl of 1× Laemmli sample buffer and 30 μl were used for WB. The raw densitometric data were expressed as ratio of Bcl10 to CaNA in Fig. 4A,B, and as ratio of Bcl10 to p-Ser band intensities in Fig. 4C,D. The ratios then were expressed as fold of increase as compared to control samples.

For total lysates, cells were treated with $A\beta_{42}$ for 48–60 h, scraped in IP buffer and total proteins were quantified. About 30–50 μg of total proteins were resolved in 5–12% gradient sodium dodecyl sulphate-polyacrylamide gel electrophoresis (SDS-PAGE) and blotted onto nitrocellulose membrane (GE Healthcare, Milan, Italy). Densitometric analysis was performed with Quantity One v. 4.6 software (Bio-Rad, Hercules, CA).

Human Material

The subjects included in this study were selected from the databases of the Departments of Neuropathology of the Academic Medical Center, University of Amsterdam (The Netherlands). Informed consent was obtained for the use of brain tissue and for access to medical records for research purposes. Tissue was obtained and used in a manner compliant with the Declaration of Helsinki. We included six hippocampal specimens of patients with AD (Braak stage V and VI) and six hippocampal specimens obtained at autopsy from controls (without evidence of degenerative changes, and lacking a clinical history of cognitive impairment; Table 1). All AD cases were pathologically staged according to Braak and Braak criteria (Braak et al., 2006). All autopsies were performed within 24 h after death.

Tissue Preparation

One or two representative paraffin blocks per case (hippocampus) were sectioned, stained, and assessed. Formalin fixed, paraffin-embedded tissue was sectioned at 6 μm and mounted on pre-coated glass slides (Star Frost, Waldemar Knittel GmbH, Braunschweig, Germany). Sections of all specimens were processed for haematoxylin eosin (HE), luxol fast blue (LFB), and Nissl stains as well as for immunocytochemical stainings for a number of markers described below.

Immunohistochemistry

Glial fibrillary acidic protein (GFAP; polyclonal rabbit, DAKO, Glostrup, Denmark; 1:4,000), neuronal nuclear protein (NeuN; mouse clone MAB377, IgG1; Chemicon, Temecula, CA; 1:1,000), human leukocyte antigen (HLA)-DP, DQ, DR (HLA-DR; major histocompatibility complex class II, MHC-II; mouse clone CR3/43; DAKO, Glostrup, Denmark, 1:400), Aβ (Mouse clone 6F/3D; DAKO; 1:200), phosphorylated Tau (pTau; mouse clone AT8; Innogenetics, Alpharetta, GA; 1:5,000) were used in the routine immunocytochemical analysis.

TABLE 1: Cases Included in this Study

Patients	Sex	Age	Braak's Neurofibrillary Staging	Clinical Diagnosis
1	M	89	V	Alzheimer's disease
2	F	77	V	Alzheimer's disease
3	F	90	V	Alzheimer's disease
4	F	70	VI	Alzheimer's disease
5	M	81	VI	Alzheimer's disease
6	F	88	VI	Alzheimer's disease
7	M	86	–	NC
8	M	91	–	NC
9	F	87	–	NC
10	M	79	–	NC
11	M	84	–	NC
12	F	76	–	NC

M = male; F = female; Braak's neurofibrillary staging: stage II–VI; NC = normal controls (without evidence of degenerative changes, and lacking a clinical history of cognitive impairment). Summary of clinical and neuropathological data of Alzheimer's disease and control patients.

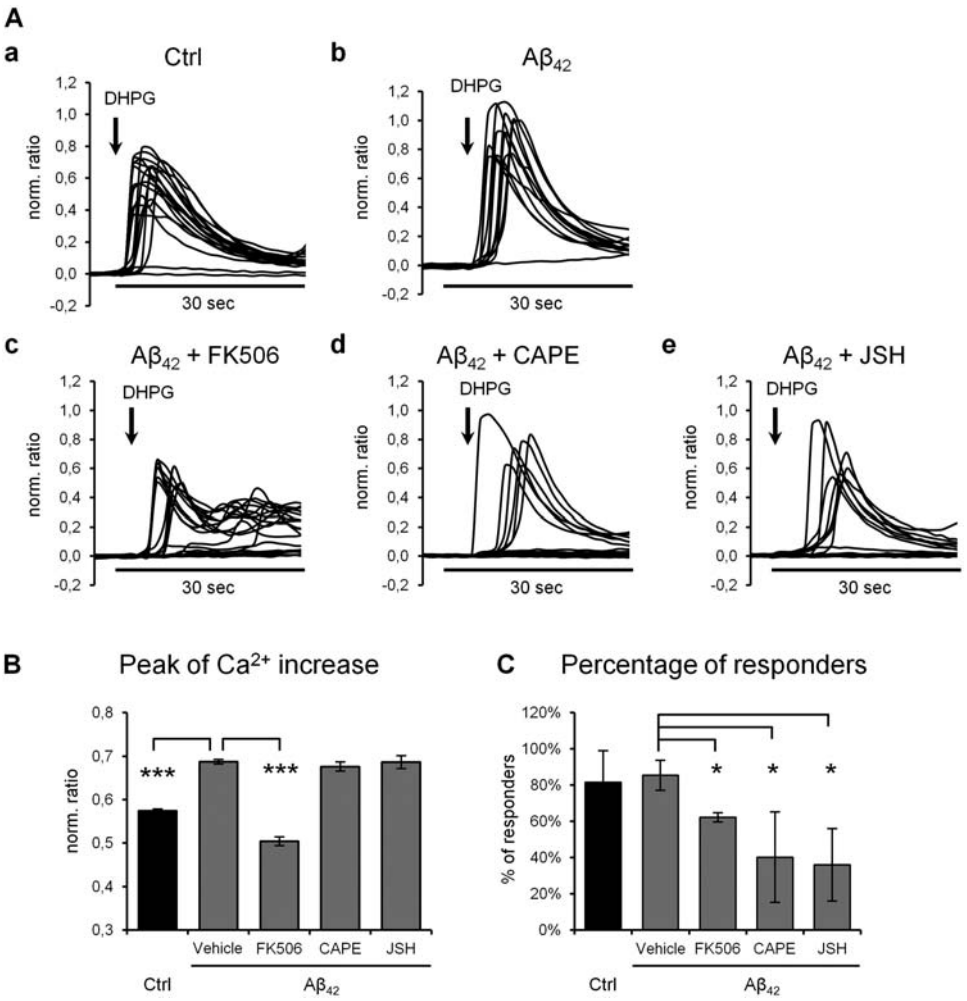

FIGURE 1: Aβ_{42}-induced up-regulation of astrocyte calcium signaling is CaN and NF-kB-dependent. (A) Primary glial cultures were pre-treated with DMSO, FK506, CAPE, or JSH for 1 h and then either non-stimulated (a) or stimulated with 100 nM Aβ_{42} (b–e) for 48 h. Representative experiments for each condition are shown. (B) Summarizing histograms of Ca^{2+}-peaks of responding cells (Norm.Fura.Ratio > 0.2) expressed as mean ± SEM; (C) Summarizing Histogram illustrating the percentage of responding cells for each condition (mean ± SD).

For the detection of mGluR5 we used two antibodies (polyclonal rabbit ab53090, from Abcam, 1:100; polyclonal rabbit from Upstate Biotechnology, Lake Placid, NY; 1:100). For the detection of p65 we used a polyclonal rabbit (sc-372; Santa Cruz; 1:50) and for the detection of CaNAα a polyclonal goat (sc-6123, Santa Cruz; 1:50) was used. Immunohistochemistry was carried out as previously described (Aronica et al., 2003). Single-label immunohistochemistry was developed using the Powervision kit (Immunologic, Duiven, The Netherlands) with 3,3-diaminobenzidine (Sigma, St. Louis, USA) as chromogen.

For double-labeling sections were incubated with Brightvision poly-alkaline phosphatase (AP)-anti-Rabbit (Immunologic, Duiven, The Netherlands) for 30 min at room temperature, and washed with PBS. Sections were washed with Tris-HCl buffer (0.1 M, pH 8,2) to adjust the pH. AP activity was visualized with the alkaline phosphatase substrate kit I Vector Red (SK-5100, Vector laboratories Inc., CA). To remove the first primary antibody sections were incubated at 121°C in citrate buffer (10 mM NaCi, pH 6.0) for 10 min. Incubation with the second primary antibody was performed overnight at 4°C. Sections with primary antibody other than rabbit were incubated with post antibody blocking from the Brightvision+ system (containing rabbit-α-mouse IgG; Immunologic, Duiven, The Netherlands). AP activity was visualized with the AP substrate kit III Vector Blue (SK-5300, Vector laboratories, CA). Sections incubated without the primary Abs or with the primary antibodies, followed by heating treatment were essentially blank.

For the double-label immunofluorescent staining, after incubation with the primary antibodies overnight at 4°C, incubated for 2h at room temperature with Alexa Fluor® 568-conjugated anti-rabbit and Alexa Fluor® 488 anti-mouse IgG or anti-goat IgG (1:100, Molecular Probes, The Netherlands). Sections were mounted with Vectashield containing DAPI (targeting DNA in the cell nucleus; blue emission) and analyzed by means of a laser scanning confocal microscope (Leica TCS Sp2, Wetzlar, Germany). Sections were then analyzed by means of a laser scanning confocal microscope (Leica TCS Sp2, Wetzlar, Germany).

RESULTS

Aβ$_{42}$-Induced Up-regulation of Astroglial Calcium Signaling is Calcineurin and NF-kB-Dependent

In the first instance, we performed Fura-2 measurements of Ca^{2+} transients induced by the mGluR agonist DHPG (20 μM) in astrocytes pretreated with the CaN inhibitor FK506 and stimulated with Aβ_{42} for 48–60 h. As shown in Fig. 1, Aβ_{42} significantly augmented the amplitude of the DHPG-induced Ca^{2+} transient (Fig. 1A(b)) as compared to control cells (Fig. 1A(a)). Pre-treatment with FK506 reduced significantly the peak of the Ca^{2+} transient and reduced significantly also the fraction of cells responding to DHPG (Fig. 1B).

Recent publications have described CaN-dependent activation of NF-kB in the immune system (Frischbutter et al., 2011; Palkowitsch et al., 2011). Furthermore, analysis of the promoter regions of the mGluR5 gene revealed no presence of NFAT binding site, a direct classical downstream CaN target, but of an NF-kB binding site, present in the second of three active promoter regions (Corti et al., 2003). We thus performed identical experiments using two inhibitors of NF-kB nuclear translocation, namely CAPE and JSH. Pretreatment with CAPE and JSH did not reduce significantly the Ca^{2+} peak amplitude, but dramatically reduced the fraction of responding astrocytes (Fig. 1A(d),B). Thus, it is plausible that alterations of mGluR5 signaling, induced by Aβ_{42}, are controlled by CaN but also by NF-kB.

Aβ$_{42}$-Induced CaN-Mediated Up-regulation of mGluR5 and IP$_3$R2 is NF-kB-Dependent, but Up-regulation of IP$_3$R1 Is Not

Treatment of astrocytes with Aβ_{42} induced a significant increase in mGluR5 expression (Fig. 2A). Pretreatment with inhibitors of both CaN and NF-kB abrogated Aβ_{42}-induced up-regulation of mGluR5 at both the mRNA (Fig. 2A(a)) and protein levels (Fig. 2A(b)). Previously, we demonstrated that both neuronal and glial splice variants of IP_3R1 were up-regulated in glial cells in a CaN-dependent manner (Grolla et al., 2013). Thus, we investigated whether Aβ_{42}-induced over-expression of IP_3R1 was also dependent on NF-kB activation. Figure 2B(a) shows that both FK506 and CsA restored the effect of Aβ_{42} on IP_3R1 mRNA levels, but both inhibitors of nuclear NF-kB translocation, CAPE and JSH, failed to do so. The data therefore support the notion that this receptor is regulated by the direct CaN target NFAT (Graef et al., 1999; Groth and Mermelstein, 2003). In astrocytes, however, IP_3R2 is the dominant isoform of the IP_3 receptors (Sharp et al., 1999). Thus, we decided to analyze IP_3R2 expression by real-time PCR. IP_3R2 was up-regulated by Aβ_{42} treatment and inhibitors of both CaN and NF-kB were able to abolish this up-regulation (Fig. 2B(b)).

Aβ$_{42}$-Induced Calcineurin Activation in Astrocytes is Calcium Dependent

Next, we investigated possible mechanisms by which Aβ_{42} may activate CaN and then NF-kB. Several possibilities have been proposed, including the incorporation of the Aβ_{42} peptide in the plasma membrane and the formation of a pore permeable to cations (Kawahara and Kuroda, 2000) or the activation by Aβ_{42} of calpain, which in turn can cleave and activate CaN (Abdul et al., 2011). Furthermore, Aβ was shown to produce Ca^{2+} oscillations in astrocytes in mixed neuronal/glial cultures (Abramov et al., 2004). We therefore investigated whether Aβ could lead to cytosolic calcium increases in glial cells. In our hands, acute Aβ_{42} treatment (up to 1 μM) in primary glial cultures did not produce any notable change in cytosolic Ca^{2+} concentrations in the first hour of treatment (data not shown). Yet, after 4–6 h of treatment, cells treated with 100 nM Aβ displayed a statistically significant increase in free cytosolic Ca^{2+} (Fig. 3A(a)). As shown in Fig. 3A(b), this significant increase was not homogeneous, but was given by a sub-group of astrocytes which increased basal Ca^{2+} to 100–150 nM. Pre-incubation with the calcium chelator BAPTA-AM abolished the elevation of cytosolic [Ca^{2+}] (data not shown). Next we investigated the effect of BAPTA on Aβ_{42}-induced up-regulation of mGluR5 mRNA. One hour pre-incubation with BAPTA-AM completely abolished mGluR5 mRNA up-regulation induced by Aβ_{42} (Fig. 3B(a)). The same result was obtained for IP_3R1 and IP_3R2 genes (Fig. 3B(b,c)), indicating that elevation of cytosolic [Ca^{2+}] is required for the activation of CaN.

We next used a range of Ca^{2+} channel blockers to investigate whether we could pin-point the source of the Ca^{2+}-increase. Neither nifedipine (100 nM) nor DNQX (30 μM) had a significant effect (data not shown), while 2-APB (100 μM) blocked such up-regulation for all three genes, mGluR5, IP_3R1, and IP_2R2 (Fig. 3B), indicating that TRP channels may be implicated in Aβ_{42}-induced elevation of cytosolic [Ca^{2+}]. Yet, 2-APB has been shown to be a rather non-specific inhibitor, and it is therefore difficult to draw conclusions.

Calcineurin Interacts with and De-phosphorylates Bcl10 in Aβ$_{42}$-Treated Glial Cells

In the immune system, it has recently been reported that CaN interacts with and de-phosphorylates B cell lymphoma 10 (BCL10) and this leads to activation of NF-kB (Frischbutter et al., 2011; Palkowitsch et al., 2011). Therefore, we investigated whether the two major CaN isoforms, CaNAα and CaNAβ, interact with Bcl10 and whether this interaction results in de-phosphorylation of Bcl10. Figure 4A,B shows that both CaNAα and CaNAβ interact with Bcl10 when CaNAα or CaNAβ were immunoprecipitated using

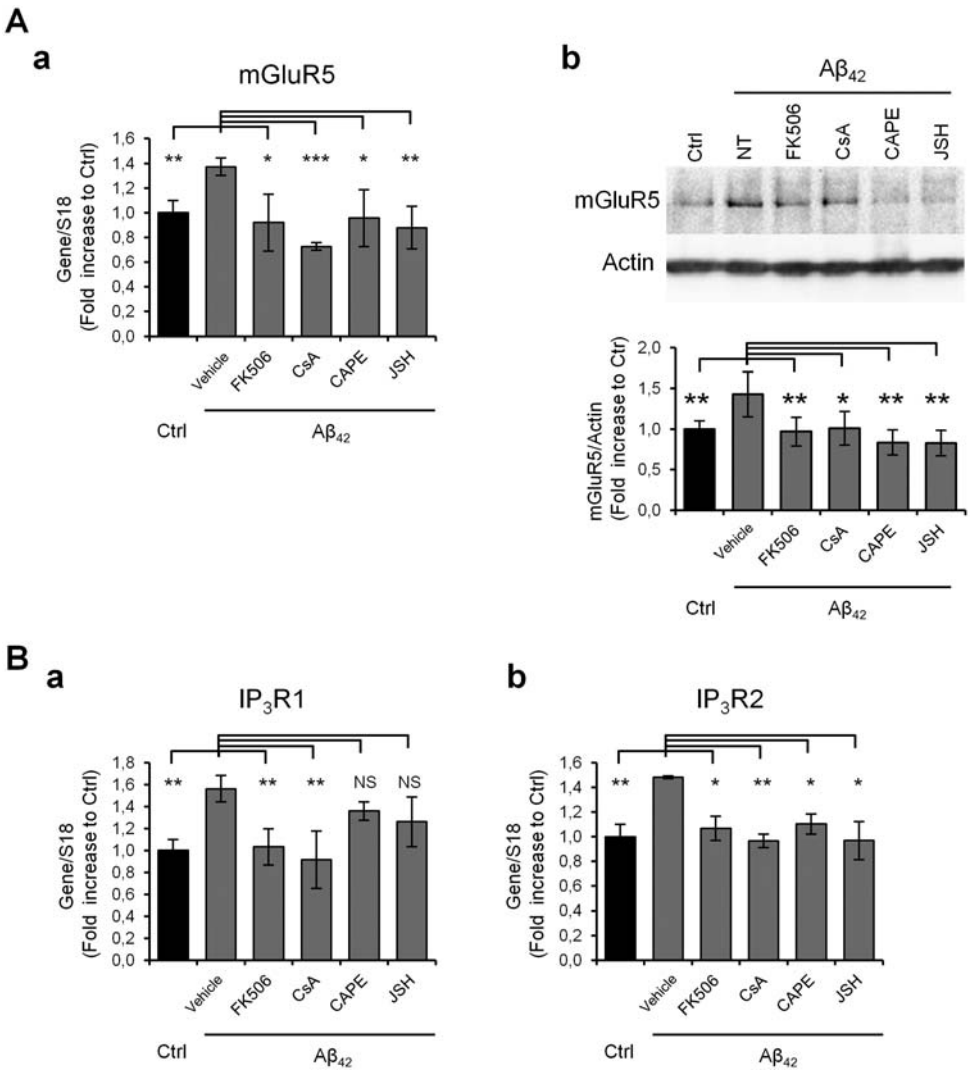

FIGURE 2: Aβ_{42}-induced and CaN-mediated up-regulation of mGluR5 and IP$_3$R2 is NF-kB-dependent, but up-regulation of IP$_3$R1 is not. (A) Real-time PCR (a) and WB analysis (b) of mGluR5 in primary glial cultures stimulated with Aβ_{42} for 24 h or 48 h, respectively. (B) Real-time PCR of IP$_3$R1 and IP$_3$R2 in primary glial cultures stimulated with Aβ_{42} for 24 h. Data were normalized to S18 ribosomal protein subunit mRNA or actin and expressed as mean ± SD reported to control. Data are from at least five independent cultures performed in triplicate (RT-PCR) or from three independent cultures (WB). *$P < 0.05$; **$P < 0.01$; ***$P < 0.001$.

isoform-specific antibodies. Moreover, densitometric analysis revealed that CaNA/Bcl10 interaction is augmented in Aβ_{42}-treated glial cultures. Interestingly, both CaN inhibitors, FK506 and CsA, significantly attenuated the interaction of Bcl10 with CaNAα, the most expressed isoform of CaNA, in Aβ_{42}-treated cells, while neither FK506 nor CsA had any significant effect on Bcl10 interaction with CaNAβ. Similar results were obtained when glial lysates were immunoprecipitated with anti-Bcl10 antibody and precipitates were probed with anti-CaNAα or anti-CaNAβ antibodies (Fig. 4C). To assess de-phosphorylation of Bcl10 by CaN, we first immunoprecipitated the lysates with anti-Bcl10 antibody and then probed precipitates with antibody recognizing phosphorylated serine residues (p-Ser). To normalize intensities of the bands the ratio Bcl10/p-Ser was used for statistical tests. As shown in Fig. 4D, Aβ_{42} significantly increased Bcl10/p-Ser ratio indicating augmented of Bcl10 de-phosphorylation. This effect was completely reversed by FK506 and attenuated by CsA. These data indicate that in glial cells CaN may activate NF-kB through de-phosphorylation of Bcl10.

Calcineurin Mediates Aβ_{42}-Induced NF-kB Activation and p65 Nuclear Translocation in Astrocytes

Next, we investigated whether Aβ_{42}-induced activation of CaN may result in nuclear translocation of NF-kB. Figure 5A shows that the NF-kB-Luc reporter gene was significantly activated by Aβ_{42} treatment. The effect was abolished when

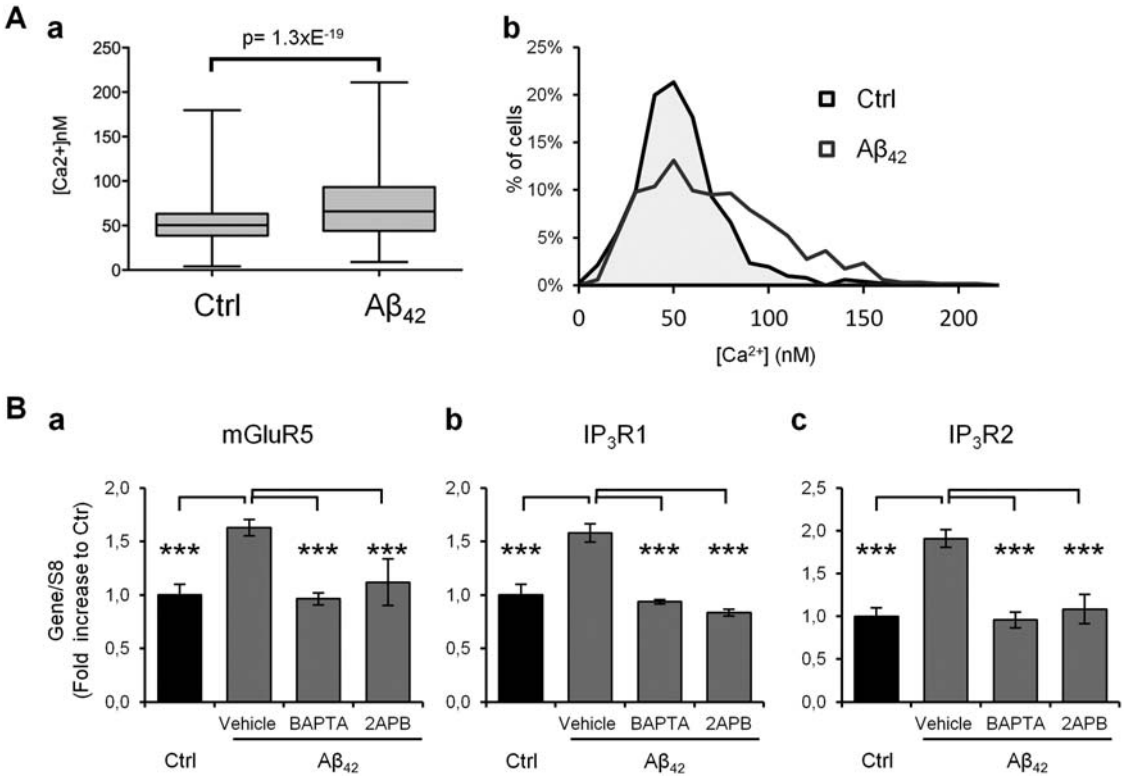

FIGURE 3: Cytosolic Ca^{2+} elevation is required for the $A\beta_{42}$-induced CaN activation. (A) Whisker box graph (a) representing mean ± SD of 515 control cells and 694 cells stimulated with $A\beta_{42}$ for 4–6 h from two independent cell preparations (12 coverslips each) and frequency distribution plot (b) of baseline Ca^{2+} concentration in control and $A\beta_{42}$-treated cells. (B) Real-time PCR of the indicated genes in cells pre-treated for 2 h with 5 μM BAPTA-AM or 100 μM 2-APB prior to $A\beta_{42}$ addition for 24 h. Data were normalized to S18 ribosomal protein subunit mRNA or actin and expressed as mean ± SD reported to control. All differences are significant at $P < 0.001$ for three independent experiments.

cells were pretreated with FK506, CsA, CAPE, or JSH. Then, we performed ICC to visualize accumulation of p65 NF-kB subunit in the nuclear compartment. As shown in Fig. 5B,C, stimulation with $A\beta_{42}$ for 5–9 h resulted in a clear nuclear localization of p65 in 42.7 ± 8.4% of astrocytes which is significantly more than in control cells (11.3 ± 3.01%, $P < 0.001$). Blockers of both CaN and NF-kB strongly inhibited translocation of p65 to the nucleus, confirming the results obtained using the NF-kB-luc reporter.

mGluR5 is Up-regulated in Astrocytes Located Close to Aβ Plaques in AD Patient's Hippocampus

In adult control hippocampus, mGluR5 is expressed throughout the CA pyramidal cells. No detectable immunoreactivity (IR) was observed in glial cells (Fig. 6A,B). In AD hippocampus, strong mGluR5 IR was detected throughout the different hippocampal regions, particularly around Aβ deposits associated with pTAU positive dystrophic neurites (Fig. 6C–F). Double labeling experiments confirmed the increased expression of mGluR5 in astrocytes (GFAP positive cells) of AD patients in proximity of Aβ plaques (Fig. 6D–H). Only occasionally co-localization with a microglial marker (HLA-DR) was observed (not shown). Double labeling with p65 and CaNAα showed co-localization with mGluR5 in astrocytes of AD hippocampus (Fig. 6I–J).

DISCUSSION

In the present study, we have investigated the effects of $A\beta_{42}$ oligomers on the astroglial signaling cascade, which includes CaN, mGluR5, and IP_3 receptors. Our principal findings are: (1) in hippocampal astrocytes, activation of CaN by $A\beta_{42}$ requires elevation of cytosolic $[Ca^{2+}]$ via Ca^{2+} entry from the extracellular milieu; (2) CaN activation leads to nuclear translocation of the transcription factor NF-kB, possibly via dephosphorylation of Bcl10, that up-regulates expression of both mGluR5 and IP_3R2; (3) a similar pathway involving CaN, but not NF-kB, controls IP_3R1 expression; and (4) these transcriptional changes have repercussions on mGluR5 activation and calcium homeostasis in glial cells. We also provide evidence that this pathway may be relevant to AD: in the hippocampus of AD patients, mGluR5 is found to be over-expressed in concomitance with over-expression of CaNAα and with p65 NF-kB subunit in GFAP-positive astrocytes located in proximity to Aβ aggregates. These data

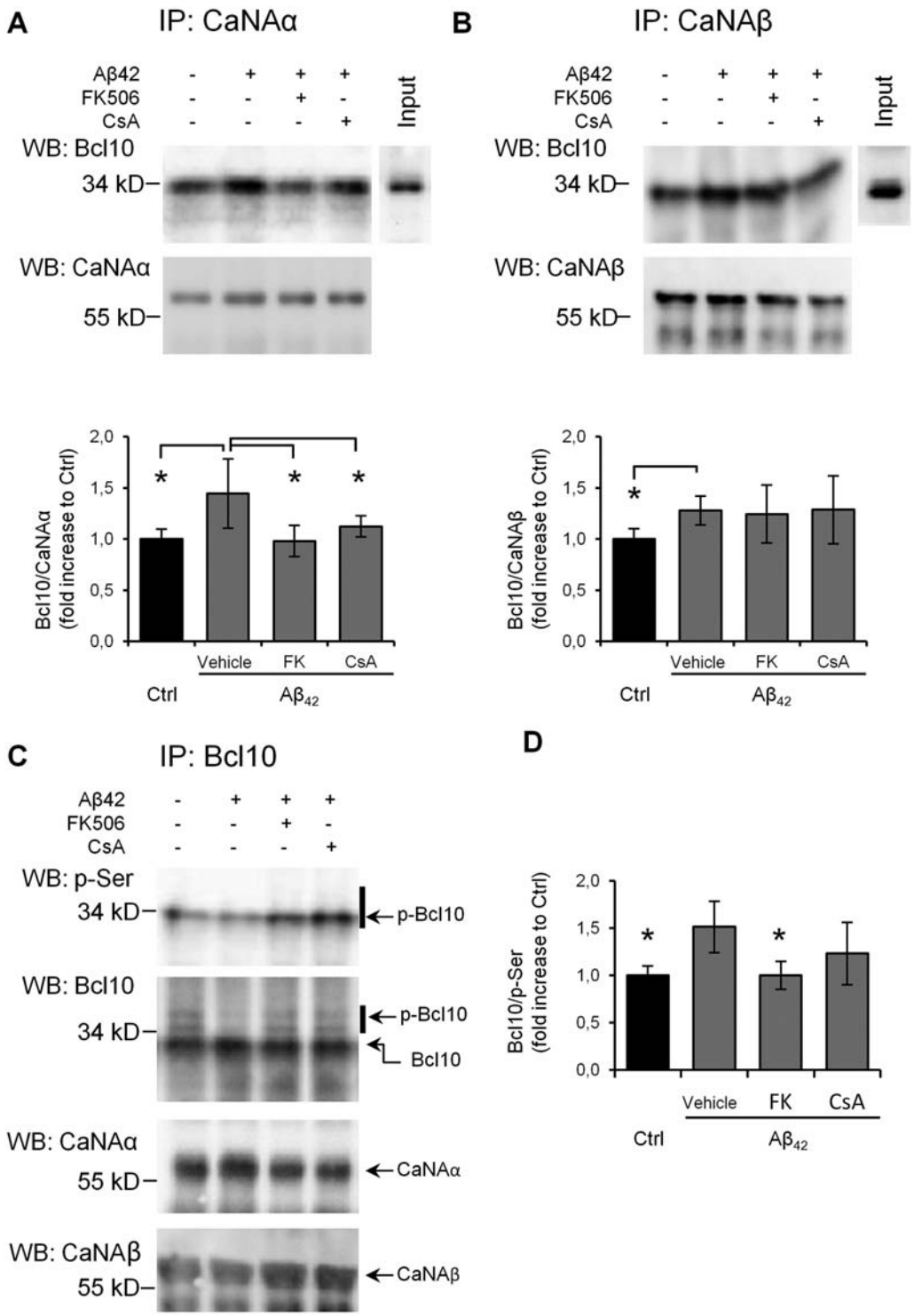

FIGURE 4: CaN interacts with and de-phosphorylates Bcl10 in Aβ_{42}-treated glial cells. (A, B) Representative results and densitometric analysis of the effect of Aβ_{42}, FK506, or CsA on the interaction of Bcl10 with CaNAα and with CaNAβ. Lysates of primary glial cultures treated with Aβ_{42} for 5 h were immunoprecipitated with anti-CaNAα and anti-CaNAβ primary antibody. Precipitates were probed with anti Bcl10 antibodies (upper bands) and with anti-CaNA (lower bands). Data in histograms are expressed as ratio of Bcl10/CaN, expressed as mean ± SD and reported to control. The differences are significant at $P < 0.05$ for three independent IP for each condition. (C) Representative results and densitometric analysis of the effect of Aβ_{42}, FK506, or CsA on the de-phosphorylation of Bcl10 and interaction with CaNAα and with CaNAβ. After 5 h of incubation with Aβ_{42}, cells were lysed and immunoprecipitated with primary anti-Bcl10 antibody. The precipitates were probed with anti-phospho serine (p-Ser), anti-Bcl10, anti-CaNAα, and anti CaNAβ primary antibodies. (D) The Bcl10/p-Ser ratios are expressed as mean ± SD and reported to control. Differences are significant at $P < 0.05$ for 6 IPs from three independent glial cultures.

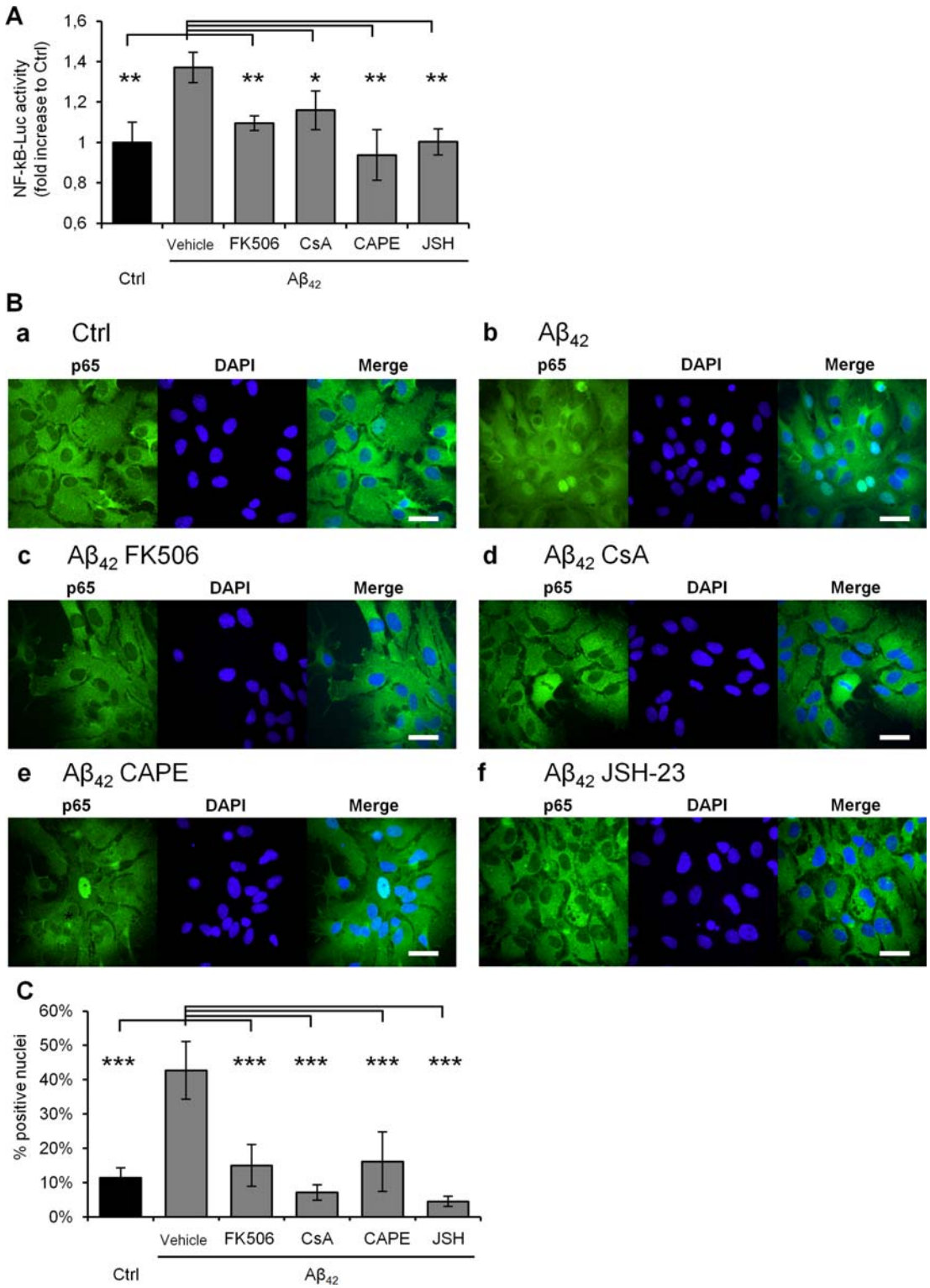

FIGURE 5: CaN mediates Aβ_{42}-induced NF-kB activation and p65 nuclear translocation in astrocytes. (A) NF-kB-Luc reporter assays in cells treated with FK506, CsA, CAPE, or JSH 1 h prior to stimulation with Aβ_{42} for 18 h. Data are expressed as mean ± SD of fold increase of luciferase activity of samples over control in five independent experiments performed in triplicate. (B) Immunocytochemical analysis of nuclear translocation of p65 subunit of NF-kB of primary astrocytes preincubated with the indicated compounds and stimulated with Aβ_{42}. Cells were fixed after 6 h of Aβ_{42} treatment, permeabilized and stained with primary anti-p65 antibody followed by 488-Alexa conjugated secondary antibody (green). Nuclei were counterstained with DAPI (blue). (C) Quantification of nuclear staining of NF-kB from six coverslips (10 fields each) from three independent experiments. Data show mean ± SD, all differences were significant at $P < 0.001$. Scale bar in (B) 25 μm.

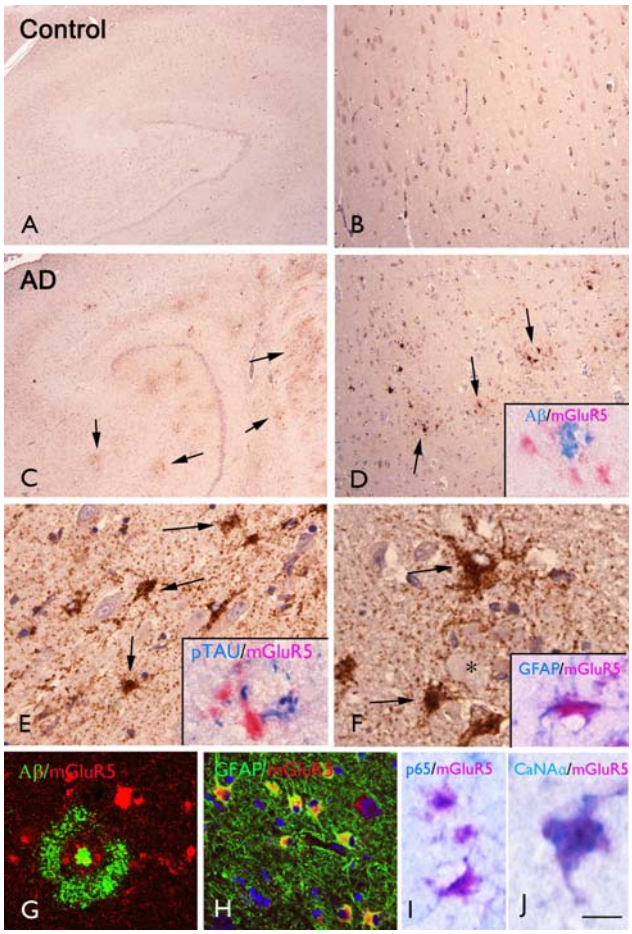

FIGURE 6: mGluR5 is up-regulated in astrocytes located close to Aβ plaques in AD patients. Panels A, B control hippocampus with expression of mGluR5 throughout the CA pyramidal cells (CA1 is shown in panel B). Panels C–J: Alzheimer' s disease (AD; stage VI) showing increased expression throughout the hippocampus, around amyloid plaques (arrows; CA1 is shown in panel D); insert in D shows mGluR5 positive cells around Aβ immunoreactivity. Panel E: strong mGluR5 immunoreactivity (IR) in astrocytes is observed in the CA1 around pyramidal neurons (arrows); insert in E shows mGluR5 positive cells around dystrophic neurites (expressing hyperphosphorylated tau; pTAU), associated with an amyloid plaque. Panel F shows high magnification of mGluR5 positive astrocytes (arrows) around an amyloid plaque (asterisk); insert in F shows expression of mGluR5 in an astrocyte (GFAP positive cell). Panel G: confocal image showing expression of mGluR5 (red) around Aβ deposits (green). Panel H: confocal image showing co-localization (yellow) of mGluR5 (red) with GFAP (green). Panels I and J: co-localization (purple) of mGluR5 with p65 (I) and calcineurin α (CaNAα; J). Scale bar in A, C: 400 μm; B, D: 160 μm; E, G, H: 40 μm; F, I: 25 μm; J: 20 μm.

are in line with previous report by Norris et al. (2005) describing CaN-immunoreactive astrocytes surrounding amyloid plaques in APP/PS1 Tg mice. We therefore propose the signaling cascade illustrated in Fig. 7.

It should be acknowledged that while our claim is that the data presented is relevant to AD, there is still controversy on whether Aβ is the key driver of the disease, or whether it

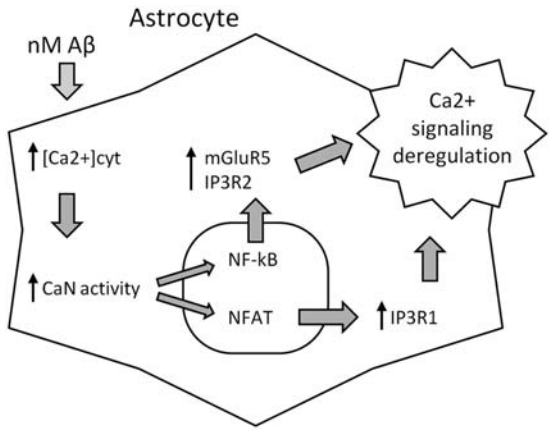

FIGURE 7: Scheme of the proposed mechanism of the Aβ-induced deregulation of Ca^{2+} signaling in astrocytes.

represents a corollary phenomenon, for example of a more generalized protein mis-processing (Aguzzi and Haass, 2003). Furthermore, it remains to be ascertained whether Aβ induces a specific astrocyte activation or whether other astrocyte insults are able to induce similar effects. Therefore, a re-arrangement of the calcium signaling machinery via CaN could be a specific phenomenon linked to AD or might have a more general function in reactive astrocytes or astrogliosis.

Furthermore, while the obvious context of our experiments would be placed around an increase in Aβ from neurons, we and others have previously shown that Aβ can be produced by astroglia (Bettegazzi et al., 2011; Grolla et al., 2013; Rossner et al., 2005). In this context, our experiments could also support a primary pivotal role of astroglia in the pathogenesis of the disease, as suggested by others (Kulijewicz et al., 2012; Yeh et al., 2011). Indeed, early astrocyte atrophy has been reported in a mouse model of AD (Rodriguez and Verkhratsky, 2011; Verkhratsky et al., 2012).

Independently of these considerations, there is an increasing evidence that CaN is involved in AD pathogenesis (Reese and Taglialatela, 2011). Activation of CaN specifically in astrocytes has been proposed to have a role in AD and in other pathological conditions (Abdul et al., 2009; Fernandez et al., 2012; Furman et al., 2012; Grolla et al., 2013; Jin et al., 2012; Norris et al., 2005; Sama et al., 2008) although the mechanisms of its activation remain largely unknown. CaN could be directly activated by calcium entering via channel-like structures formed by Aβ (Kagan and Thundimadathil, 2010), via Ca^{2+}-permeable channels on the plasma membrane modulated by Aβ (Pellistri et al., 2008), or indirectly via the cleavage of the CaNA auto-inhibitory domain by calpain (Abdul et al., 2011). In our experiments, we used nanomolar [$A\beta_{42}$], compatible with the [Aβ] found in the cerebro-spinal fluid of AD patients (Mehta et al., 2001). We report that the acute treatment of cultured astrocytes with

100 nM Aβ_{42} did not change baseline [Ca^{2+}] for up to 1 h of recording. However, when cells were taken for Ca^{2+} imaging 4–6 h after Aβ_{42} addition, a fraction of cells had elevated [Ca^{2+}]cyt in a range of 100–150 nM, which is in line with [Ca^{2+}]cyt necessary to activate CaN in cerebellar granule neurons (Guerini et al., 1999). Abdul et al. (2009) reported nuclear translocation of NFAT-EGFP reporter already 15 min after addition of similar [Aβ], indicating that in their experiment Aβ-induced CaN activation occurred significantly earlier than in our experiments. At least two factors may account for this discrepancy: (i) different procedures of preparation of Aβ which could affect effective concentration oligomeric Aβ; and (ii) different protocols of preparations primary astroglial cultures. Furthermore, all CaN-dependent changes in mRNA expression were abolished by clamping cytosolic Ca^{2+}, and indicate that involvement of cation channels is possible in the Aβ_{42}-induced Ca^{2+} entry. Last, we find that 2-APB, a nonspecific cation blocker abolishes the effect.

CaN inhibitors have been widely used as immunosuppressants and most of their actions can be reconciled with inhibition of NFAT-dependent transcription (Lee and Burckart, 1998). Astroglial CaN-NFAT signaling has been characterized by several groups (Canellada et al., 2008; Furman et al., 2010; Pérez-Ortiz et al., 2008; Sama et al., 2008). Recently, it was proposed that CaN is an essential for activation of NF-kB in immune cells (Frischbutter et al., 2011; Palkowitsch et al., 2011) where Bcl10, a member of the so called CBM complex, interacts with and is de-phosphorylated by CaN to recruit other two CBM members, mucosa-associated lymphoid tissue lymphoma translocation protein 1 (MALT1) and caspase recruitment domain membrane-associated guanylate kinase protein 1 (CARMA1) in a ternary complex, whose downstream effects are degradation of IkB and nuclear translocation of NF-kB. This may therefore constitute a parallel pathway that mediates CaN's actions in the immune system. Thus, we decided to investigate whether CaN interacts with Bcl10 also in glial cells. We found that, in fact, this was the case. Both CaNAα and CaNAβ co-immunoprecipitated with Bcl10 in glial cultures. Moreover, in our experiments, stimulation with Aβ_{42} significantly augmented this interaction in which Bcl10 was also de-phosphorylated. As the effect of CaN and NF-kB inhibitors overlap in our experiments for mGluR5 and IP_3R2, we propose this pathway as being responsible. Yet, it has been proposed also that, in astrocytes, CaN activates NF-kB via interaction with Forkhead box O (FoxO) transcription factor 3 (Foxo3) in TNFα-stimulated cells (Fernandez et al., 2012). Interestingly, Foxo3 may also be activated downstream of Bcl10 and Ikk signaling cascade (Luron et al., 2012).

The Ca^{2+}-CaN-NF-kB pathway activation, in our system, leads to a profound remodeling of Ca^{2+}-handling capacity of astrocytes. As such, it might be suggested that, in AD brains, this would lead to profound changes in astroglial Ca^{2+}-dependent processes, including gliotransmission and reactive inflammation. As such, these could participate actively in the pathogenesis of the disease.

In support of the occurrence of these phenomena in AD, we also show that in hippocampi from human AD brains, mGluR5 was over-expressed with CaNAα in GFAP-positive astrocytes in proximity to amyloid plaques and co-localized with p65.

Acknowledgment

Authors thank Dr. Colin Taylor for anti-IP_3R1 antibody and Dr. Christian Zurlo for the help in maintenance of animals. They are grateful to J.J. Anink for his technical help. Authors declare no conflict of interests.

References

Abdul HM, Baig I, Levine H III, Guttmann RP, Norris CM. Proteolysis of calcineurin is increased in human hippocampus during mild cognitive impairment and is stimulated by oligomeric Abeta in primary cell culture. Aging Cell 2011;10:103–113.

Abdul HM, Sama MA, Furman JL, Mathis DM, Beckett TL, Weidner AM, Patel ES, Baig I, Murphy MP, LeVine H III, Kraner SD, Norris CM. Cognitive decline in Alzheimer's disease is associated with selective changes in calcineurin/NFAT signaling. J Neurosci 2009;29:12957–12969.

Abramov AY, Canevari L, Duchen MR. Calcium signals induced by amyloid beta peptide and their consequences in neurons and astrocytes in culture. Biochim Biophys Acta 2004;1742:81–87.

Aguzzi A, Haass C. Games played by rogue proteins in prion disorders and Alzheimer's disease. Science 2003;302:814–818.

Aronica E, Gorter JA, Jansen GH, van Veelen CW, van Rijen PC, Ramkema M, Troost D. Expression and cell distribution of group I and group II metabotropic glutamate receptor subtypes in taylor-type focal cortical dysplasia. Epilepsia 2003;44:785–795.

Bettegazzi B, Mihailovich M, Di Cesare A, Consonni A, Macco R, Pelizzoni I, Codazzi F, Grohovaz F, Zacchetti D. Beta-Secretase activity in rat astrocytes: Translational block of BACE1 and modulation of BACE2 expression. Eur J Neurosci 2011;33:236–243.

Braak H, Alafuzoff I, Arzberger T, Kretzschmar H, Del Tredici K. Staging of Alzheimer disease-associated neurofibrillary pathology using paraffin sections and immunocytochemistry. Acta Neuropathol 2006;112:389–404.

Canellada A, Ramirez BG, Minami T, Redondo JM, Cano E. Calcium/calcineurin signaling in primary cortical astrocyte cultures: Rcan1–4 and cyclooxygenase-2 as NFAT target genes. Glia 2008;56:709–722.

Corti C, Clarkson RW, Crepaldi L, Sala CF, Xuereb JH, Ferraguti F. Gene structure of the human metabotropic glutamate receptor 5 and functional analysis of its multiple promoters in neuroblastoma and astroglioma cells. J Biol Chem 2003;278:33105–33119.

Demuro A, Parker I, Stutzmann GE. Calcium signaling and amyloid toxicity in Alzheimer disease. J Biol Chem 2010;285:12463–12468.

DeWitt DA, Perry G, Cohen M, Doller C, Silver J. Astrocytes regulate microglial phagocytosis of senile plaque cores of Alzheimer's disease. Exp Neurol 1998;149:329–40.

Fernandez AM, Jimenez S, Mecha M, Dávila D, Guaza C, Vitorica J, Torres-Aleman I. Regulation of the phosphatase calcineurin by insulin-like growth factor I unveils a key role of astrocytes in Alzheimer's pathology. Mol Psychiatry 2012;17:705–718.

Fresu L, Dehpour A, Genazzani AA, Carafoli E, Guerini D. Plasma membrane calcium ATPase isoforms in astrocytes. Glia 1999;28:150–155.

Frischbutter S, Gabriel C, Bendfeldt H, Radbruch A, Baumgrass R. Dephosphorylation of Bcl-10 by calcineurin is essential for canonical NF-κB activation in Th cells. Eur J Immunol 2011;41:2349–2357.

Furman JL, Artiushin IA, Norris CM. Disparate effects of serum on basal and evoked NFAT activity in primary astrocyte cultures. Neurosci Lett 2010;469: 365–369.

Furman JL, Sama DM, Gant JC, Beckett TL, Murphy MP, Bachstetter AD, Van Eldik LJ, Norris CM. Targeting astrocytes ameliorates neurologic changes in a mouse model of Alzheimer's disease. J Neurosci 2012;32:16129–16140.

Giuffrida ML, Caraci F, Pignataro B, Cataldo S, De Bona P, Bruno V, Molinaro G, Pappalardo G, Messina A, Palmigiano A, Garozzo D, Nicoletti F, Rizzarelli E, Copani A. Beta-amyloid monomers are neuroprotective. J Neurosci 2009; 29:10582–10587.

Graef IA, Mermelstein PG, Stankunas K, Neilson JR, Deisseroth K, Tsien RW, Crabtree GR. L-type calcium channels and GSK-3 regulate the activity of NF-ATc4 in hippocampal neurons. Nature 1999;401:703–708.

Grolla AA, Fakhfouri G, Balzaretti G, Marcello E, Gardoni F, Canonico PL, Diluca M, Genazzani AA, Lim D. Aβ leads to Ca(2+) signaling alterations and transcriptional changes in glial cells. Neurobiol Aging 2013;34:511–522.

Groth RD, Mermelstein PG. Brain-derived neurotrophic factor activation of NFAT (nuclear factor of activated T-cells)-dependent transcription: A role for the transcription factor NFATc4 in neurotrophin-mediated gene expression. J Neurosci 2003;23:8125–8134.

Grynkiewicz G, Poenie M, Tsien RY. A new generation of Ca2+ indicators with greatly improved fluorescence properties. J Biol Chem 1985;260: 3440–3450.

Guerini D, García-Martin E, Gerber A, Volbracht C, Leist M, Merino CG, Carafoli E. The expression of plasma membrane Ca2+ pump isoforms in cerebellar granule neurons is modulated by Ca2+. J Biol Chem 1999;274: 1667–1676.

Hardy J, Selkoe DJ. The amyloid hypothesis of Alzheimer's disease: Progress and problems on the road to therapeutics. Science 2002;297:353–356.

Jin SM, Cho HJ, Kim YW, Hwang JY, Mook-Jung I. Aβ-induced Ca(2+) influx regulates astrocytic BACE1 expression via calcineurin/NFAT4 signals. Biochem Biophys Res Commun 2012;425:649–655.

Kagan BL, Thundimadathil J. Amyloid peptide pores and the beta sheet conformation. Adv Exp Med Biol 2010;677:150–167.

Kawahara M, Kuroda Y. Molecular mechanism of neurodegeneration induced by Alzheimer's beta-amyloid protein: Channel formation and disruption of calcium homeostasis. Brain Res Bull 2000;53:389–397.

Kuchibhotla KV, Goldman ST, Lattarulo CR, Wu HY, Hyman BT, Bacskai BJ. Abeta plaques lead to aberrant regulation of calcium homeostasis in vivo resulting in structural and functional disruption of neuronal networks. Neuron 2008;59:214–225.

Kuchibhotla KV, Lattarulo CR, Hyman BT, Bacskai BJ. Synchronous hyperactivity and intercellular calcium waves in astrocytes in Alzheimer mice. Science 2009;323:1211–1215.

Kulijewicz-Nawrot M, Verkhratsky A, Chvátal A, Syková E, Rodríguez JJ. Astrocytic cytoskeletal atrophy in the medial prefrontal cortex of a triple transgenic mouse model of Alzheimer's disease. J Anat 2012;221:252–262.

Lee JI, Burckart GJ. Nuclear factor kappa B: Important transcription factor and therapeutic target. J Clin Pharmacol 1998;38:981–993.

Luron L, Saliba D, Blazek K, Lanfrancotti A, Udalova IA. FOXO3 as a new IKK-ε-controlled check-point of regulation of IFN-β expression. Eur J Immunol 2012;42:1030–1037.

Marcello E, Gardoni F, Mauceri D, Romorini S, Jeromin A, Epis R, Borroni B, Cattabeni F, Sala C, Padovani A, Di Luca M. Synapse-associated protein-97 mediates alpha-secretase ADAM10 trafficking and promotes its activity. J Neurosci 2007;27:1682–1691.

Mehta PD, Pirttila T, Patrick BA, Barshatzky M, Mehta SP. Amyloid beta protein 1–40 and 1–42 levels in matched cerebrospinal fluid and plasma from patients with Alzheimer disease. Neurosci Lett 2001;304:102–106.

Norris CM, Kadish I, Blalock EM, Chen KC, Thibault V, Porter NM, Landfield PW, Kraner SD. Calcineurin triggers reactive/inflammatory processes in astrocytes and is upregulated in aging and Alzheimer's models. J Neurosci 2005;25:4649–4658.

Palkowitsch L, Marienfeld U, Brunner C, Eitelhuber A, Krappmann D, Marienfeld RB. The Ca2+-dependent phosphatase calcineurin controls the formation of the Carma1-Bcl10-Malt1 complex during T cell receptor-induced NF-kappaB activation. J Biol Chem 2011;286:7522–7534.

Parpura V, Heneka MT, Montana V, Oliet SH, Schousboe A, Haydon PG, Stout RFJr, Spray DC, Reichenbach A, Pannicke T, Pekny M, Pekna M, Zorec R. Glial cells in (patho)physiology. J Neurochem 2012;121:4–27.

Pellistri F, Bucciantini M, Relini A, Nosi D, Gliozzi A, Robello M, Stefani M. Nonspecific interaction of prefibrillar amyloid aggregates with glutamatergic receptors results in Ca2+ increase in primary neuronal cells. J Biol Chem 2008;283:29950–29960.

Pérez-Ortiz JM, Serrano-Pérez MC, Pastor MD, Martín ED, Calvo S, Rincón M, Tranque P. Mechanical lesion activates newly identified NFATc1 in primary astrocytes: Implication of ATP and purinergic receptors. Eur J Neurosci 2008; 27:2453–2465.

Peters O, Schipke CG, Philipps A, Haas B, Pannasch U, Wang LP, Benedetti B, Kingston AE, Kettenmann H. Astrocyte function is modified by Alzheimer's disease-like pathology in aged mice. J Alzheimers Dis 2009;18:177–189.

Reese LC, Taglialatela G. A role for calcineurin in Alzheimer's disease. Curr Neuropharmacol 2011;9:685–692.

Rodríguez JJ, Verkhratsky A. Neuroglial roots of neurodegenerative diseases?Mol Neurobiol 2011;43:87–96.

Rossner S, Lange-Dohna C, Zeitschel U, Perez-Polo JR. Alzheimer's disease beta-secretase BACE1 is not a neuron-specific enzyme. J Neurochem 2005; 92:226–234.

Rubio-Perez JM, Morillas-Ruiz JM. A review: Inflammatory process in Alzheimer's disease, role of cytokines. Sci World J 2012;2012:756357.

Sama MA, Mathis DM, Furman JL, Abdul HM, Artiushin IA, Kraner SD, Norris CM. Interleukin-1beta-dependent signaling between astrocytes and neurons depends critically on astrocytic calcineurin/NFAT activity. J Biol Chem 2008; 283:21953–21964.

Sharp AH, Nucifora FCJr, Blondel O, Sheppard CA, Zhang C, Snyder SH, Russell JT, Ryugo DK, Ross CA. Differential cellular expression of isoforms of inositol 1,4,5-triphosphate receptors in neurons and glia in brain. J Comp Neurol 1999;406:207–220.

Supnet C, Bezprozvanny I. The dysregulation of intracellular calcium in Alzheimer disease. Cell Calcium 2010;47:183–189.

Thibault O, Gant JC, Landfield PW. Expansion of the calcium hypothesis of brain aging and Alzheimer's disease: Minding the store. Aging Cell 2007;6: 307–317.

Tu H, Nelson O, Bezprozvanny A, Wang Z, Lee SF, Hao YH, Serneels L, De Strooper B, Yu G, Bezprozvanny I. Presenilins form ER Ca2+ leak channels, a function disrupted by familial Alzheimer's disease-linked mutations. Cell 2006;126:981–993.

Verkhratsky A, Sofroniew MV, Messing A, deLanerolle NC, Rempe D, Rodríguez JJ, Nedergaard M. Neurological diseases as primary gliopathies: A reassessment of neurocentrism. ASN Neuro 2012;4:art:e00082.

Yeh CY, Vadhwana B, Verkhratsky A, Rodríguez JJ. Early astrocytic atrophy in the entorhinal cortex of a triple transgenic animal model of Alzheimer's disease. ASN Neurol 2011;3:271–279.